


RESEARCH ARTICLE

Corpus callosum axon diameter relates to cognitive impairment in multiple sclerosis

Susie Y. Huang¹, Qiuyun Fan¹, Natalya Machado², Ani Eloyan³, John D. Bireley², Andrew W. Russo², Sean M. Tobyne², Kevin R. Patel² , Kristina Brewer², Sarah F. Rapaport², Aapo Nummenmaa¹, Thomas Witzel¹, Janet C. Sherman⁴, Lawrence L. Wald¹ & Eric C. Klawiter²

¹Athinoula A. Martin Center for Biomedical Imaging, Department of Radiology, Massachusetts General Hospital, Charlestown, Massachusetts

²Department of Neurology, Massachusetts General Hospital, Boston, Massachusetts

³Department of Biostatistics, School of Public Health, Brown University, Providence, Rhode Island

⁴Psychology Assessment Center, Department of Neurology, Massachusetts General Hospital, Boston, Massachusetts

Correspondence

Susie Y. Huang, Division of Neuroradiology, Department of Radiology, Massachusetts General Hospital, 55 Fruit Street, GRB-273A, Boston, MA 02129. Tel: +1 617-643-7319; Fax: +1 617-724-3338; E-mail: syhuang@partners.org
and

Eric C. Klawiter, Department of Neurology, Massachusetts General Hospital, 15 Parkman Street, Boston, MA 02114. Tel: +1 617-726-4094; Fax: +1 617-726-7422; E-mail: eklawiter@mgh.harvard.edu

Funding Information

This work was supported by National Institutes of Health (NIH) (K23NS096056 to S.Y.H., K23NS078044 to E.C.K., R00EB015445 to A.N., P41EB015896), the National Multiple Sclerosis Society (E.C.K., K.R.P.), the Radiological Society of North America and Conrad N. Hilton Foundation (S.Y.H.), and an American Heart Association Postdoctoral Fellowship (Q.F.).

Received: 7 December 2018; Revised: 16 February 2019; Accepted: 27 February 2019

Annals of Clinical and Translational Neurology 2019; 6(5): 882–892

doi: 10.1002/acn3.760

Introduction

Cognitive dysfunction is common in multiple sclerosis (MS), occurring in approximately 50% of patients with MS, and is a major contributor to disability and loss of employment.¹ Cognitive impairment occurs early in the disease course, predominantly in the domains of information processing speed and episodic memory.² Despite its

Abstract

Objective: To evaluate alterations in apparent axon diameter and axon density obtained by high-gradient diffusion MRI in the corpus callosum of MS patients and the relationship of these advanced diffusion MRI metrics to neurologic disability and cognitive impairment in MS. **Methods:** Thirty people with MS (23 relapsing-remitting MS [RRMS], 7 progressive MS [PMS]) and 23 healthy controls were scanned on a human 3-tesla (3T) MRI scanner equipped with 300 mT/m maximum gradient strength using a comprehensive multishell diffusion MRI protocol. Data were fitted to a three-compartment geometric model of white matter to estimate apparent axon diameter and axon density in the midline corpus callosum. Neurologic disability and cognitive function were measured using the Expanded Disability Status Scale (EDSS), Multiple Sclerosis Functional Composite (MSFC), and Minimal Assessment of Cognitive Function in MS battery. **Results:** Apparent axon diameter was significantly larger and axon density reduced in the normal-appearing corpus callosum (NACC) of MS patients compared to healthy controls, with similar trends seen in PMS compared to RRMS. Larger apparent axon diameter in the NACC of MS patients correlated with greater disability as measured by the EDSS ($r = 0.555$, $P = 0.007$) and poorer performance on the Symbol Digits Modalities Test ($r = -0.593$, $P = 0.008$) and Brief Visuospatial Memory Test–Revised ($r = -0.632$, $P < 0.01$), tests of interhemispheric processing speed and new learning and memory, respectively. **Interpretation:** Apparent axon diameter in the corpus callosum obtained from high-gradient diffusion MRI is a potential imaging biomarker that may be used to understand the development and progression of cognitive impairment in MS.

impact, the pathophysiology and neural basis underlying the progression of cognitive decline in MS is still largely unknown.³ Structural disconnection of the corpus callosum due to axonal damage is thought to contribute to the development of cognitive dysfunction.⁴ Corpus callosum atrophy has been widely appreciated in MS and correlates with the level of cognitive impairment.⁵ Alterations in diffusion tensor imaging (DTI) metrics

have implicated tissue damage in the corpus callosum,^{6,7} although the specificity of these findings for inflammatory demyelination and axonal damage is limited. In general, MS lesions show increased mean diffusivity (MD) and decreased fractional anisotropy (FA) compared with normal white matter,⁸ and changes in MD and FA are associated with demyelination as well as axonal loss.⁹ However, direct comparisons of DTI measures with histopathology from *ex vivo* MS spinal cord samples have shown that radial diffusivity and FA reflect demyelination to a greater extent than axonal loss.¹⁰ The limitations of currently available diffusion MRI methods motivate the development of techniques to improve pathologic specificity.

Recent improvements in gradient hardware¹¹ have enabled the clinical application of advanced diffusion MRI methods such as AxCaliber¹² for estimating axonal size and density in the corpus callosum *in vivo*.^{11,13,14} Advanced diffusion MRI metrics that are sensitive and specific to axonal integrity offer a unique opportunity to study the alterations in axonal size and density that occur in MS noninvasively and alongside tests of functional status, with potentially greater specificity than more conventional approaches such as DTI. Despite the demanding acquisition and limited availability of such systems, the motivation for using such advanced hardware, sequences and models for diffusion MRI is to improve the understanding of the pathophysiology and microstructural substrate of the progressive disability that develops in MS. It is important to note that axon diameter estimation based on compartment models of diffusion MRI data represents a proportional estimate of the axon diameter and not the true axon diameter. Therefore, throughout this paper, we refer to the estimated quantity as “apparent axon diameter.”

Previous postmortem studies of the central nervous system in MS patients have detected widespread axonal loss and an overall increase in average axon diameter in the normal-appearing white matter and lesions.^{4,15–17} Although the exact mechanism underlying this shift toward larger axon diameter is not known, it has been hypothesized that small diameter axons are more vulnerable to axonal injury following demyelination.^{16,18,19}

In this study, we applied high-gradient diffusion MRI to evaluate the relationship between axonal pathology in the corpus callosum and the level of disability and cognitive dysfunction in MS. We hypothesized that an overall increase in apparent axon diameter and decrease in axon density would be observed in the corpus callosum of MS patients compared to healthy controls based on the selective vulnerability of small diameter axons to axonal damage, and that the degree of alteration in apparent axon diameter and axon density in the corpus callosum would correlate with greater levels of disability and cognitive impairment affecting domains relying on interhemispheric function.

Methods

Subjects

This study was approved by the institutional review board. All participants provided written informed consent. MS patients were recruited prospectively from the Massachusetts General Hospital MS Clinic between July 2015 and March 2018. Thirty MS subjects (23 relapsing-remitting MS [RRMS], 5 secondary progressive MS [SPMS], and two primary progressive MS [PPMS]) were enrolled. Twenty-three age-matched healthy individuals served as controls. Inclusion criteria for MS patients were: a diagnosis of clinically definite MS, absence of clinical relapse within 3 months, and being on stable disease-modifying treatment or no treatment for at least 6 months. Exclusion criteria were: other major medical and/or psychiatric disorders, severe claustrophobia, presence of non-MRI compatible implants/devices, and other MRI contraindications.

All patients with MS completed a battery of clinical and neuropsychological tests based on the Minimal Assessment of Cognitive Function in MS (MACFIMS)²⁰ battery and Multiple Sclerosis Functional Composite (MSFC).²¹ A board- and EDSS-certified neurologist blinded to imaging and neuropsychological test performance conducted a standard clinical examination, which was used in the calculation of the EDSS. Neuropsychological testing was administered by a trained examiner within 1 week of the MRI scan. Neuropsychological tests included the Symbol Digit Modalities Test (SDMT), the California Verbal Learning Test, the Brief Visual Memory Test–Revised (BVMT-R), the Paced Auditory Serial Addition Test, the Controlled Oral Word Association Test, the Delis-Kaplan Executive Function System Sorting Test, and the Benton Judgment of Line Orientation Test. The MSFC *z*-score was calculated using the SDMT, timed 25-foot walk, and timed 9-hole peg test.²² MRI data in healthy volunteers were acquired as part of a separate technical development study, and neuropsychological testing was not performed in these subjects.

MRI data acquisition

All subjects were scanned on the dedicated high-gradient (AS302) 3 Tesla MRI scanner (MAGNETOM CONNEC-TOM, Siemens Healthcare, Erlangen, Germany) with a maximum gradient strength of 300 mT/m. A single diffusion MRI acquisition protocol was implemented in all subjects. This multishell acquisition consisted of two diffusion times ($\Delta = 19$ msec and 49 msec) and eight gradient strengths per diffusion time, which were linearly spaced from 30 to 290 mT/m, resulting in a total of 16 *b*-values for the entire acquisition. The diffusion-encoding parameters for this single diffusion MRI acquisition

protocol are listed in Table 1, including the diffusion times, diffusion gradient pulse duration, gradient strengths, number of diffusion-encoding gradient directions, and b -values. The diffusion-weighted images were acquired with spatial resolution of $2 \times 2 \times 2 \text{ mm}^3$ voxels, echo time (TE)/repetition time (TR)=77/3600 msec, parallel imaging acceleration factor $r = 2$, simultaneous multislice imaging with a slice acceleration factor of 2, and anterior-to-posterior phase encoding. Interspersed $b = 0$ images were acquired every 16 images. In addition, a set of 5 $b = 0$ images with reversal of the phase encoding direction was acquired separately to correct for geometric distortions due to susceptibility effects. The diffusion MRI protocol was optimized to fit within an hour of total scan time. The diffusion MRI acquisition protocol was designed to include the minimum number of diffusion-weighted imaging volumes to obtain reproducible estimates of apparent axon diameter and density compared to a more extensive acquisition,²³ while keeping the scan time within a reasonable duration for imaging patients. The total acquisition time for the diffusion MRI protocol was 51 min, with the 32-direction diffusion acquisitions lasting 2 min 2 sec each and the 64-direction diffusion acquisitions lasting 4 min 5 sec each.

Structural sequences included a high-resolution three-dimensional T1-weighted (T1w) multiecho magnetization-prepared rapid gradient echo (MEMPRAGE) sequence [TR/TE=2530/[1.15, 3.03, 4.89, 6.75], inversion time (TI)=1100 msec, $1 \times 1 \times 1 \text{ mm}^3$ voxels, $r = 2$] and three-dimensional fluid-attenuated inversion recovery (FLAIR) images [TE/TR/TI=389/5000/1800 msec, $0.9 \times 0.9 \times 0.9 \text{ mm}^3$ voxels, $r = 2$], which were used for registration and segmentation.

MRI data analysis

Data preprocessing and quality control

We used the data preprocessing pipeline established for the MGH-USC Human Connectome project²⁴ using tools

Table 1. Diffusion-encoding parameters used in the multidiffusion time, multigradient strength diffusion MRI protocol.

Δ (msec)	δ (msec)	Gradient strengths (mT/m)	# of	
			Gradient directions	b -values (sec/mm^2)
19	8	31, 68, 105, 142	32	50, 350, 800, 1500
		179, 216, 253, 290	64	2400, 3450, 4750, 6000
49	8	31, 68, 105	32	200, 950, 2300
		142, 179, 216, 253, 290	64	4250, 6750, 9850, 13500, 17800

Abbreviations: Δ , diffusion time; δ , diffusion-encoding pulse duration.

from the FreeSurfer²⁵ (<http://surfer.nmr.mgh.harvard.edu>) and FMRIB Software Library²⁶ (FSL, <https://fsl.fmrib.ox.ac.uk>) toolboxes. Following preprocessing, all diffusion-weighted MRI data underwent quality assessment by a multirater team, which included a trained neuroradiologist, postdoctoral researcher, and research assistant. Each dataset was assessed by at least two raters, who evaluated both the unprocessed and preprocessed data volume by volume, and rated each in terms of head movement, susceptibility-induced distortion, and eddy current correction. Of the scans performed, approximately 5% of the diffusion volumes were discarded, largely due to the presence of excessive motion.

Fitting for diffusion MRI metrics

Diffusion in the corpus callosum was modeled as occurring in three compartments: restricted diffusion within axons, hindered diffusion in the extra-axonal space, and free diffusion in cerebrospinal fluid (CSF), following previously proposed approaches for modeling diffusion in white matter.^{12,27} The parameters estimated in the three-compartment model included: apparent axon diameter, relative volume fractions of water within the restricted intra-axonal space and CSF (referred to here as the restricted and CSF volume fractions), and diffusivity of water in the hindered extra-axonal space (referred to here as the hindered diffusivity). These parameters were obtained by fitting the corrected multidiffusion time, multigradient strength diffusion MRI data to a previously validated three-compartment model of intra-axonal restricted diffusion, extra-axonal hindered diffusion, and free diffusion.^{28,29}

Model fitting was performed on a voxel-wise basis using Markov chain Monte Carlo (MCMC) sampling. MCMC simulations provided samples of the posterior distributions of the model parameters given the data. The restricted diffusion coefficient D_r was set to $1.7 \mu\text{m}^2/\text{msec}$, which is comparable to the estimated in vivo axial diffusivity in white matter and in keeping with values used in prior studies.^{13,27} The diffusion coefficient of CSF was assumed to be that of free water ($3 \mu\text{m}^2/\text{msec}$). A Rician noise model was adopted for parameter estimation.^{27,30} The mean estimates for apparent axon diameter, restricted and CSF volume fractions, and hindered diffusivity were calculated for each voxel by taking the mean over the MCMC samples. The axon density was calculated by weighting the restricted fraction by the cross-sectional area calculated using the mean apparent axon diameter, as described previously.^{27,31}

DTI metrics of MD and FA were calculated by applying the DTIFIT tool in FSL using an ordinary least-squares fit to the diffusion MRI data acquired at $b = 800 \text{ sec}/\text{mm}^2$

with a diffusion time of 19 msec and 32 diffusion-encoding gradient directions.

Corpus callosum and lesion segmentation

Cortical surface reconstruction and volumetric segmentation was performed on the T1w images of all MS patients and healthy controls using the FreeSurfer automated surface reconstruction and analysis package (version 5.3, <http://surfer.nmr.mgh.harvard.edu/>).^{32,33} The FreeSurfer toolbox was chosen for its ability to provide accurate parcellation of the subcortical white matter and its pre-existing implementation in our data preprocessing pipeline. A corpus callosum mask was created from the FreeSurfer label for the corpus callosum and manually edited to ensure exclusion of voxels outside the corpus callosum (e.g., fornix and CSF). The mid-sagittal and next adjacent parasagittal slices of the corpus callosum were selected for each subject to ensure that the corpus callosum, lesion, and normal-appearing corpus callosum (NACC) masks included corpus callosum fibers with the greatest fiber coherence.

Lesion segmentation was performed on the FLAIR images of all MS patients. The FLAIR images were first registered to the T1w data using the boundary-based registration tool in FreeSurfer. T2-hyperintense lesions were manually segmented on the FLAIR images by a board- and subspecialty-certified neuroradiologist and subtracted from the corpus callosum masks to generate NACC masks for all MS patients.

The average of the interleaved $b = 0$ images after susceptibility correction was registered to the T1w data, and the FreeSurfer labels in native T1w image space were transformed into diffusion image space using the inverse of the diffusion-to-native T1w image transformation. Summary statistics were extracted from the parameter maps using the corpus callosum, lesion, and NACC masks (Fig. 1).

Atrophy of the corpus callosum was assessed as an additional clinically relevant conventional measure related to cognitive function and disability in MS. Volumetric measures of the corpus callosum suffer from imprecise delineation of the lateral margins of the corpus callosum. Here, we applied a recently developed method for measuring corpus callosum area in the mid-sagittal plane.^{34,35} In brief, intensity normalization was applied to the T1w data, which was then registered to MNI152 atlas space using a 6 degree of freedom rigid body transformation performed with FSL's Linear Image Registration Tool (FLIRT).³⁶ The images were then segmented by tissue type using FMRIB's Automated Segmentation Tool (FAST v.4),³⁷ including partial volume estimation (PVE). The mid-sagittal slice of the white matter PVE map was

extracted from the whole volume, thresholded to remove voxels that contained less than 30% of white matter and binarized to produce a mid-sagittal white matter map. The white matter map was manually edited to remove any remaining noncallosal white matter (e.g., fornix and brainstem). The area of the mid-sagittal corpus callosum was then calculated by summing the remaining voxels. The corpus callosum area normalized for head size by dividing by the estimated total intracranial volume ($eTIV$)^(2/3) as calculated by FreeSurfer.³⁴

Statistical analysis

Statistical calculations were performed using R (R Foundation for Statistical Computing, Vienna, Austria). Student's t tests, χ^2 tests, or Wilcoxon rank-sum tests were used as indicated, following the Shapiro–Wilk test for normality. Individual correlations between disability scores (EDSS and MSFC-3) as well as neuropsychological test scores from the MACFIMS and the MRI metrics of apparent axon diameter, restricted volume fraction, axon density, FA, MD and corpus callosum area were assessed adjusting for age, sex, and years of education. A multiple linear regression model was also used to assess the relative influence of the MRI metrics of apparent axon diameter, restricted volume fraction, FA, MD, and normalized corpus callosum area in MS patients to predict disability scores (EDSS and MSFC-3) and neuropsychological test scores adjusting for age, sex, and years of education. Correction for multiple comparisons based on the false discovery rate (FDR) was applied with the FDR threshold set at 0.05. The raw uncorrected P -values surviving FDR correction are reported here.

Results

Clinical characteristics

This study included a total of 30 patients with MS and 23 healthy control subjects. Demographic information, disability scores, and neuropsychological test scores are presented in Table 2. The MS group as a whole did not differ significantly from the healthy control group in age or sex ratio. Furthermore, the RRMS subjects did not differ significantly from the combined progressive MS subgroup in age, sex, disease duration, education, or use of disease-modifying therapy, as many of the progressive MS patients were treated with disease-modifying therapy despite their progressive status. Disability as measured by the EDSS and MSFC-3 (SDMT) was significantly worse in the progressive MS subjects compared to RRMS. Mean neuropsychological test scores in several domains tested by the MACFIMS, including processing speed and

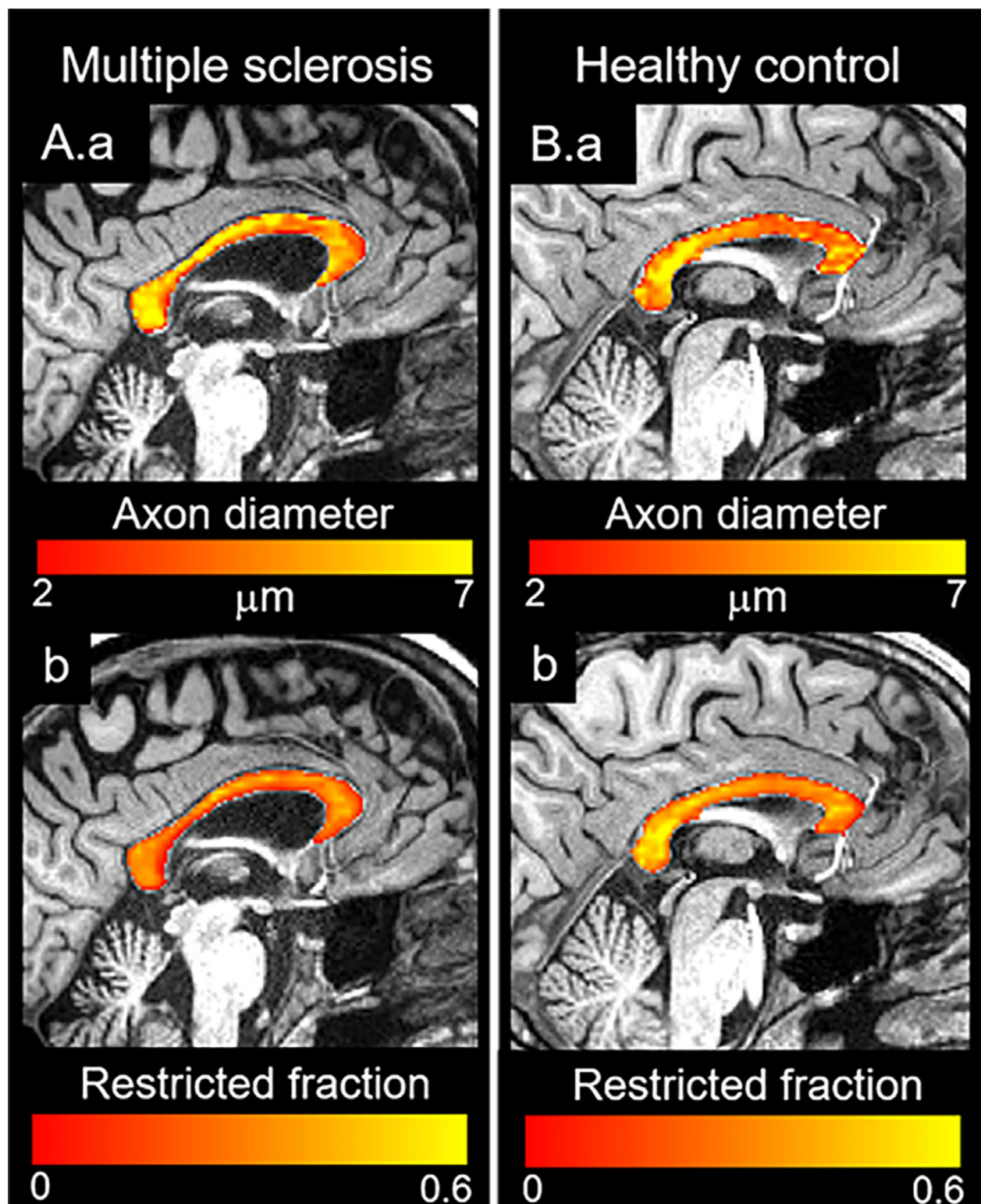


Figure 1. Axon diameter and restricted volume fraction maps in the corpus callosum using high-gradient diffusion MRI. Sagittal axon diameter and restricted volume fraction maps in the midline corpus callosum show diffusely increased axon diameter and decreased restricted fraction in a patient with multiple sclerosis (A.a and b) compared to an age-matched healthy control (B.a and b).

Table 2. Demographics and clinical data.

	HC (n = 23)	Total MS (n = 30)	RRMS (n = 23)	Progressive MS (n = 7)	MS versus HC ¹ P-value	RRMS versus progressive MS P-value
Demographics						
Age, y, mean ± SD [range]	40.2 ± 11.9 [24–61]	43.9 ± 11.2 [23–60]	42.6 ± 10.6 [23–58]	48.1 ± 12.8 [26–60]	0.25 ²	0.32 ²
Female, n (%)	14 (61%)	24 (80%)	19 (83%)	5 (71%)	0.25 ³	0.52 ³
Disease duration, y, mean ± SD [range]	N/A	10.8 ± 6.7 [1–23]	10.3 ± 6.7 [1–23]	12.3 ± 6.9 [4–23]	N/A	0.52 ²
Disease-modifying therapy, n (%)	N/A	26 (87%)	21 (91%)	5 (71%)	N/A	0.27 ³
Dimethyl fumarate		8	8	0		
Glatiramer acetate		6	6	0		
β-interferons		4	3	2		
Fingolimod		3	2	1		
Natalizumab		2	2	0		
Rituximab		2	0	2		
Ocrelizumab		1	1	0		
None		4	2	2		
Education, y, mean ± SD [range]	N/A	16.4 ± 2.4 [12–23]	16.9 ± 2.4 [12–23]	14.9 ± 2.0 [11–18]	N/A	0.108 ²
Disability scores						
EDSS score, mean ± SD [range]	N/A	3.0 ± 1.9 [1–7.5]	2.1 ± 0.8 [1–3.5]	5.8 ± 1.6 [3–7.5]	N/A	0.0009 ⁴
MSFC-3, mean ± SD [range]	N/A	−0.54 ± 2.06 [−6.21–1.08]	0.30 ± 0.52 [−0.80–1.08]	−3.29 ± 2.82 [−6.21–−0.05]	N/A	0.0022 ⁴
Cognitive scores						
SDMT _{z-score}	N/A	−0.054 ± 1.44 [−2.72–3.42]	0.27 ± 1.33 [−2.72–3.42]	−1.11 ± 1.31 [−2.48–1.45]	N/A	0.02 ²
BVMT-R _{z-score}	N/A	−0.10 ± 1.39 [−3.57–1.98]	0.31 ± 1.02 [−1.78–1.98]	−1.46 ± 1.64 [−3.57–0.9]	N/A	0.0016 ²
PASAT _{z-score}	N/A	−0.45 ± 1.34 [−4.27–0.99]	−0.18 ± 1.09 [−2.93–0.99]	−1.32 ± 1.76 [−4.27–0.89]	N/A	0.11 ⁴
COWAT _{z-score}	N/A	−0.35 ± 0.99 [−2.98–1.46]	−0.30 ± 0.94 [−2.12–1.46]	−0.52 ± 1.20 [−2.98–0.58]	N/A	0.61 ²
JLO _{total}	N/A	63.3 ± 28.5 [1.5–86]	70.8 ± 22.9 [9–86]	38.4 ± 32.8 [1.5–86]	N/A	0.013 ⁴
CVLT _{total}	N/A	47 ± 14.9 [17–73]	52.9 ± 12.1 [30–73]	32.8 ± 12.6 [17–49]	N/A	0.0009 ²
DKEFS _{total}	N/A	11.5 ± 3.21 [5–17]	12.2 ± 3.16 [5–17]	9.57 ± 2.63 [5–12]	N/A	0.055 ²

Abbreviations: HC, healthy control; MS, multiple sclerosis; RRMS, relapsing-remitting multiple sclerosis; EDSS, Expanded Disability Status Scale; MSFC, Multiple Sclerosis Functional Composite; SDMT, Symbol Digit Modalities Test; BVMT-R, Brief Visual Memory Test–Revised; PASAT, Paced Auditory Serial Addition Test; COWAT, Controlled Oral Word Association Test; JLO, Benton Judgment of Line Orientation Test; CVLT, California Verbal Learning Test; DKEFS, Delis-Kaplan Executive Function System Sorting Test.

¹MS versus HC group comparisons conducted with entire MS sample.

²Student's *t*-test.

³χ²-test.

⁴Wilcoxon rank-sum test.

working memory (SDMT) and new learning and memory (BVMT-R), were significantly worse in the progressive MS subgroup.

MRI metrics in lesions versus normal-appearing corpus callosum

Of the 30 MS subjects, 10 (33%; 7 RRMS, 3 SPMS) had T2 hyperintense lesions identified in the midline corpus callosum, with lesions comprising an average of 0.6% of the total volume. Compared to the adjacent NACC, lesions showed significantly larger apparent axon diameter, lower restricted volume fraction and lower axon

density (Table 3). Fractional anisotropy was also significantly lower in lesions compared to NACC.

MRI metrics in normal-appearing corpus callosum

Apparent axon diameter in the NACC was significantly larger in MS subjects compared to healthy controls (HC) and also in progressive MS compared to RRMS (Table 4). Axon density was significantly lower in MS subjects compared to HC. Axon density was also significantly lower in progressive MS compared to RRMS. Higher MD, lower FA and lower corpus callosum area were observed in MS

Table 3. Comparison of MRI metrics in lesions versus normal-appearing corpus callosum of patients with multiple sclerosis.

	Lesion	NACC	Lesion vs. NACC	
			Test statistic	P-value
Axon diameter, μm , mean \pm SD	5.02 \pm 0.97	4.16 \pm 0.68	2.80 ¹	0.02*
Restricted volume fraction, mean \pm SD	0.19 \pm 0.04	0.27 \pm 0.07	-2.70 ¹	0.01*
Axon density, $\times 10^{10}/\text{m}^2$, mean \pm SD	3.69 \pm 2.45	7.59 \pm 4.10	-2.80 ¹	0.01*
MD, $\mu\text{m}^2/\text{msec}$, mean \pm SD	1.05 \pm 0.23	0.96 \pm 0.04	1.12 ¹	0.26
FA, mean \pm SD	0.53 \pm 0.15	0.67 \pm 0.04	-2.24 ¹	0.04

Abbreviations: NACC, normal-appearing corpus callosum; MD, mean diffusivity; FA, fractional anisotropy.

¹Wilcoxon sign-rank test. Raw uncorrected P-values are reported.

*indicates P-values that survive multiple comparison correction using the false discovery rate (FDR) with an FDR threshold of 0.05.

Table 4. Comparison of MRI metrics in normal-appearing corpus callosum of patients with multiple sclerosis versus healthy controls.

	HC (n = 23)	Total MS (n = 30)	RRMS (n = 23)	Progressive MS (n = 7)	MS versus HC ¹	RRMS versus progressive MS
					P-value	P-value
Axon diameter, μm , mean \pm SD	4.63 \pm 0.30	4.89 \pm 0.31	4.81 \pm 0.27	5.17 \pm 0.25	0.004 ^{2,*}	0.004 ^{2,*}
Restricted volume fraction, mean \pm SD	0.33 \pm 0.03	0.31 \pm 0.03	0.31 \pm 0.03	0.30 \pm 0.03	0.026 ^{2,*}	0.64 ²
Axon density, $\times 10^{10}/\text{m}^2$, mean \pm SD	7.25 \pm 0.83	6.04 \pm 1.5	6.43 \pm 0.95	5.34 \pm 0.65	0.001 ^{2,*}	0.008 ^{2,*}
MD, $\mu\text{m}^2/\text{msec}$, mean \pm SD	0.93 \pm 0.05	0.99 \pm 0.14	0.98 \pm 0.15	1.03 \pm 0.09	0.035 ^{3,*}	0.047 ³
FA, mean \pm SD	0.67 \pm 0.04	0.66 \pm 0.06	0.66 \pm 0.07	0.63 \pm 0.03	0.77 ³	0.08 ³
Corpus callosum area, mm^2 , mean \pm SD	627.4 \pm 82.5	558.5 \pm 94.7	578.5 \pm 86.4	493.1 \pm 97.0	0.007 ^{2,*}	0.03 ²
Normalized corpus callosum area, mean \pm SD	0.047 \pm 0.006	0.042 \pm 0.008	0.044 \pm 0.007	0.038 \pm 0.007	0.028 ^{2,*}	0.09 ²

Abbreviations: MD, mean diffusivity; FA, fractional anisotropy.

¹MS versus HC group comparisons conducted with entire MS sample;

²Student's *t*-test;

³Wilcoxon rank-sum test. Raw uncorrected P-values are reported throughout.

*denotes significance following correction for multiple comparisons using the false discovery rate with an FDR threshold of 0.05.

subjects compared to HC, although the significance of these trends did not survive correction for multiple comparisons.

Disability as measured by the EDSS was significantly associated with apparent axon diameter in the NACC, with larger apparent axon diameter observed in patients with higher EDSS after adjusting for the effects of age, sex, and years of education (Table 5). The associations between the NACC MRI metrics and neuropsychological tests included in the MACFIMS battery were also studied after adjusting for the effects of age, sex, and years of education, with tests showing significant associations reported in Table 5. Larger axon diameter was significantly associated with poorer performance on tests of information processing speed, specifically the SDMT, and a test of new visual learning and memory, the BVMT-R. Performances on other cognitive measures did not correlate with any of the MRI measures. Thinning of the

corpus callosum was significantly correlated with poorer performance on the EDSS.

To determine the relative contribution of the MRI metrics in explaining the degree of disability and cognitive impairment, a multiple regression analysis was performed to predict disability and neuropsychological test scores from the MRI metrics of apparent axon diameter, restricted volume fraction, MD, FA, and normalized corpus callosum area, in addition to age, sex, and years of education. Of all the imaging metrics, apparent axon diameter in the NACC of MS patients was positively correlated with EDSS ($b = 2.67$, $P = 0.044$). Apparent axon diameter in the NACC of the MS patients was negatively correlated with the SDMT ($b = -3.19$, $P = 0.0004$) and BVMT-R ($b = -2.86$, $P = 0.0025$). In the same multiple regression analysis, thinning of the corpus callosum was associated with impaired information processing speed as assessed by the SDMT ($b = -85.95$, $P = 0.009$).

Table 5. Correlation of disability and neuropsychological test scores with corpus callosum MRI metrics, adjusting for age, sex, and years of education.

	EDSS	MSFC-3 _{z-score}	SDMT _{z-score}	BVMT-R _{z-score}
Axon diameter	0.555 (0.007)*	-0.486 (0.04)	-0.593 (0.008)*	-0.632 (<0.001)*
Restricted fraction	0.100 (0.73)	-0.041 (0.59)	-0.052 (0.95)	-0.343 (0.24)
Axon density	-0.277 (0.07)	0.276 (0.12)	0.358 (0.066)	0.220 (0.11)
MD	0.121 (0.75)	-0.534 (0.06)	-0.123 (0.56)	0.030 (0.56)
FA	-0.052 (0.88)	0.157 (0.52)	0.179 (0.48)	-0.046 (0.75)
CC area	-0.460 (0.015)*	0.456 (0.024)	0.127 (0.94)	0.380 (0.042)

Abbreviations: EDSS, Expanded Disability Status Scale; MSFC, Multiple Sclerosis Functional Composite; SDMT, Symbol Digit Modalities Test; BVMT-R, Brief Visuospatial Memory Test-Revised; MD, mean diffusivity; FA, fractional anisotropy. Linear correlation coefficients are reported with *P*-values in parentheses adjusted for age, sex, and years of education. Values in parentheses represent raw uncorrected *P*-values.

*denotes significance following correction for multiple comparisons using the false discovery rate with an FDR threshold of 0.05.

The influence of disease phenotype was also studied in a separate multiple regression analysis performed in the RRMS subgroup to determine the influence of age, gender, education, and the MRI metrics of apparent axon diameter, restricted volume fraction, MD, FA and normalized corpus callosum area on disability and cognitive impairment. For the RRMS patients, apparent axon diameter was significantly correlated with EDSS ($b = 1.32$, $P = 0.016$), MSFC-3 ($b = -0.95$, $P = 0.012$), and SDMT ($b = -2.60$, $P = 0.005$). A borderline significant correlation was also found between apparent axon diameter and the BVMT-R after correcting for age, sex, and education ($b = -1.64$, $P = 0.058$). In the same multiple regression analysis, thinning of the corpus callosum was significantly associated with poorer performance on the MSFC-3 ($b = -28.00$, $P = 0.034$) and SDMT ($b = -102.74$, $P = 0.003$). Similar analyses could not be performed for the progressive MS subgroup as the sample size was too small to generate reliable statistical comparisons.

Discussion

The purpose of this study was to investigate the relationship between recently developed MRI markers of axonal pathology and disability and cognitive dysfunction in MS patients. We found significantly larger apparent axon diameter and decreased axon density in the NACC of MS subjects compared to HC and between RRMS compared to progressive MS subjects. Apparent axon diameter was the strongest and most significant predictor of disability as measured by the EDSS, as well as of poorer cognitive performance as reflected in the SDMT and BVMT-R, tests of information processing speed and working memory.

The results reported here confirm and expand upon findings from previous studies using AxCaliber and related techniques for assessing apparent axon diameter and density in MS lesions and normal-appearing white matter. Our previous pilot study using a high-gradient

diffusion MRI protocol and AxCaliber analysis found larger apparent axon diameter in lesions and NACC in a separate group of RRMS patients compared to white matter in age-matched HC.¹⁴ Another pilot study using diffusion MRI to estimate axon diameter in the corpus callosum of two MS subjects applied a machine learning approach that incorporated the effect of exchange between the intra- and extra-axonal spaces.³⁸ This study also demonstrated larger apparent axon diameter and decreased axon density in lesions within the corpus callosum compared to NACC and within the NACC compared to HC. In the current work, we studied the relationship of axon diameter and density in the corpus callosum with cognitive performance in a larger group of patients with RRMS and progressive MS, using a generalized acquisition and analysis of high-gradient diffusion MRI data,²⁸ such that the obtained microstructural metrics were independent of fiber orientation.

Our findings of larger apparent axon diameter and decreased axon density in the NACC of MS subjects are in agreement with previous neuropathological studies, which reported axonal loss in major white matter tracts such as the corpus callosum, corticospinal tracts, and spinal cord.^{15-17,19} Previous MRI/histopathologic studies in the spinal cord have found larger axon diameter and lower axon density within MS lesions compared to normal-appearing white matter in the spinal cord, with similar trends found in normal-appearing white matter of MS patients compared to healthy controls.^{39,40} In particular, small diameter axons seem to be more vulnerable to axonal injury following demyelination, resulting in a shift toward larger apparent axon diameter in both normal-appearing and lesioned white matter in the chronic phase of MS.^{16,18,19} Several hypotheses have been advanced to explain why small diameter axons may be particularly vulnerable to inflammation-mediated axonal injury. In terms of energetics, the volume-to-surface area ratio is reduced in small diameter axons, resulting in a limited

volume in which mitochondria can redistribute relative to membrane channels.⁴¹ The limited “energy-to-ions” ratio in small diameter axons has been posited to result in disproportionate axonal loss.⁴²

Our study also advances previous work by showing correlation of indices of axonal pathology with measures of disability and cognitive performance. Callosal structural integrity is associated with cognitive performance in multiple domains, including information processing speed, working memory, and episodic memory – the most frequently affected cognitive domains in MS.¹ The strong correlations between apparent axon diameter and the SDMT and BVMT-R suggest that apparent axon diameter may be a primary structural substrate of alterations in processing speed commonly seen in MS. Larger apparent axon diameter was also associated with worse performance on the EDSS. These relationships were replicated by a subanalysis in the RRMS patients alone, suggesting that the strength of the associations was not driven by the progressive MS patients but rather valid throughout the spectrum of disease, even in its earlier stages. Thinning of the corpus callosum was significantly correlated with a greater level of disability as measured by the EDSS. In addition, in the multiple regression analysis of MRI metrics and neuropsychological test scores, thinning of the corpus callosum was significantly associated with impaired information processing speed as assessed by the SDMT, in keeping with findings from prior studies.^{5,43} Overall, our results suggest that apparent axon diameter obtained from high-gradient diffusion MRI may provide clinically relevant information that may complement what can be gleaned from volumetric measures and their surrogates alone.

Overall, our findings support the hypothesis that axonal damage in the corpus callosum proceeds as a result of Wallerian degeneration of axons that are transected following demyelination elsewhere in the hemispheric white matter, with the transition from acute to progressive MS occurring when axonal loss exceeds the compensatory capacity of the brain to adapt to injury.⁴⁴ While the cross-sectional nature of this study is not sufficient to draw firm conclusions regarding the progression of clinical disability, our preliminary observations suggest that apparent axon diameter and axon density may be potential biomarkers of aspects of cognitive dysfunction and, to a lesser extent, physical disability in MS.

There are several limitations to the current study. For one, the lengthy scan time is an important practical issue in comparing our current approach to more conventional protocols. The multishell diffusion MRI protocol used here could conceivably undergo further optimization to reduce scan time even more, and newer machine learning approaches may be applied in the future to extract these

parameters more efficiently, given the presence of potentially redundant information embedded within the diffusion MRI data that may not be readily discernable using our multicompartment model. The small sample size and heterogeneity of the patient population may limit the generalizability of the findings. However, we were able to uncover statistically significant comparisons and correlations despite a relatively small sample size, which supports the promise and validity of the approach. The apparent axon diameter and axon density inferred here are only estimates of the true axon diameter and density and are subject to the limitations of the AxCaliber model. In our study, we used a simple three-compartment model of intra-axonal restricted, extra-axonal hindered, and free water diffusion to account for diffusion in both normal-appearing white matter and in MS lesions. The use of a single axon diameter or even the gamma distribution as proposed in the original AxCaliber model may not adequately capture the alterations in axonal size in the presence of axonal pathology. Furthermore, the time dependence of water diffusion in the extra-axonal space was not accounted for and could conceivably bias the estimates of axon diameter to larger values,^{45–49} although the range of diffusion times used in our study was relatively small (19–49 msec). The generally reduced axon density found in MS lesions and NACC could conceivably affect the ability to estimate apparent axon diameter using this technique, as the estimates for axon diameter become noisier with less intra-axonal water. To mitigate against this concern, we chose to perform ROI-based analyses across the midline and parasagittal slices of the corpus callosum, which are more robust to noise compared to direct voxel-based comparisons.

Despite its limitations, the current model provided a reasonable fit to the data without introducing additional a priori assumptions or free parameters. Future work should focus on developing more complex functions to model axon diameter and density within lesions based on known histopathological alterations to the white matter microstructure. Systematic validation of the advanced imaging metrics presented here against histopathology will be needed to determine whether the overall larger mean apparent axon diameter observed in MS lesions and NACC compared to HC reflects selective loss of small diameter axons or an increase in the diameter of the remaining axons.

Our current data suggest that apparent axon diameter is significantly associated with disability and aspects of cognitive performance in MS. If substantiated in larger, longitudinal studies, axonal imaging biomarkers provided by high-gradient diffusion MRI may help to elucidate the pathophysiology of the disease with implications for improving our understanding of the development of physical disability and cognitive deficits in MS.

Acknowledgments

This work was supported by National Institutes of Health (NIH) (K23NS096056 to S.Y.H., K23NS078044 to E.C.K., R00EB015445 to A.N., P41EB015896), the National Multiple Sclerosis Society (E.C.K., K.R.P.), the Radiological Society of North America and Conrad N. Hilton Foundation (S.Y.H.), and an American Heart Association Postdoctoral Fellowship (Q.F.).

Author Contributions

S.Y.H., and E.C.K studied the concept and designed the study. S.Y.H, Q.F., N.M., A.E., J.D.B., A.W.R., S.M.T., K.R.P., K.B., S.F.R., A.N., T.W., and E.C.K did data acquisition and analysis. All authors drafted the manuscript and figures.

Conflict of Interest

None declared.

References

- Rao SM, Leo GJ, Bernardin L, Unverzagt F. Cognitive dysfunction in multiple sclerosis. I. Frequency, patterns, and prediction. *Neurology* 1991;41:685–691.
- Benedict RH, Zivadinov R. Risk factors for and management of cognitive dysfunction in multiple sclerosis. *Nat Rev Neurol* 2011;7:332–342.
- Sumowski JF, Benedict R, Enzinger C, et al. Cognition in multiple sclerosis: state of the field and priorities for the future. *Neurology* 2018;90:278–288.
- Evangelou N, Konz D, Esiri MM, et al. Regional axonal loss in the corpus callosum correlates with cerebral white matter lesion volume and distribution in multiple sclerosis. *Brain* 2000;123(Pt 9):1845–1849.
- Granberg T, Martola J, Bergendal G, et al. Corpus callosum atrophy is strongly associated with cognitive impairment in multiple sclerosis: results of a 17-year longitudinal study. *Mult Scler* 2015;21:1151–1158.
- Mesaros S, Rocca MA, Riccitelli G, et al. Corpus callosum damage and cognitive dysfunction in benign MS. *Hum Brain Mapp* 2009;30:2656–2666.
- Ozturk A, Smith SA, Gordon-Lipkin EM, et al. MRI of the corpus callosum in multiple sclerosis: association with disability. *Mult Scler* 2010;16:166–177.
- Ge Y. Multiple sclerosis: the role of MR imaging. *AJNR* 2006;27:1165–1176.
- Schmierer K, Wheeler-Kingshott CA, Boulby PA, et al. Diffusion tensor imaging of post mortem multiple sclerosis brain. *NeuroImage* 2007;35:467–477.
- Klawiter EC, Schmidt RE, Trinkaus K, et al. Radial diffusivity predicts demyelination in ex vivo multiple sclerosis spinal cords. *NeuroImage* 2011;55:1454–1460.
- McNab JA, Edlow BL, Witzel T, et al. The Human Connectome Project and beyond: initial applications of 300 mT/m gradients. *NeuroImage* 2013;15:234–245.
- Assaf Y, Blumenfeld-Katzir T, Yovel Y, Basser PJ. AxCaliber: a method for measuring axon diameter distribution from diffusion MRI. *Magn Reson Med* 2008;59:1347–1354.
- Huang SY, Nummenmaa A, Witzel T, et al. The impact of gradient strength on in vivo diffusion MRI estimates of axon diameter. *NeuroImage* 2015;1:464–472.
- Huang SY, Topyne SM, Nummenmaa A, et al. Characterization of axonal disease in patients with multiple sclerosis using high-gradient-diffusion MR imaging. *Radiology* 2016;280:244–251.
- Evangelou N, Esiri MM, Smith S, et al. Quantitative pathological evidence for axonal loss in normal appearing white matter in multiple sclerosis. *Ann Neurol* 2000;47:391–395.
- Lovas G, Szilagyi N, Majtenyi K, et al. Axonal changes in chronic demyelinated cervical spinal cord plaques. *Brain* 2000;123(Pt 2):308–317.
- DeLuca GC, Ebers GC, Esiri MM. Axonal loss in multiple sclerosis: a pathological survey of the corticospinal and sensory tracts. *Brain* 2004;127(Pt 5):1009–1018.
- DeLuca GC, Williams K, Evangelou N, et al. The contribution of demyelination to axonal loss in multiple sclerosis. *Brain* 2006;129(Pt 6):1507–1516.
- Tallantyre EC, Bo L, Al-Rawashdeh O, et al. Clinico-pathological evidence that axonal loss underlies disability in progressive multiple sclerosis. *Mult Scler* 2010;16:406–411.
- Benedict RH, Cookfair D, Gavett R, et al. Validity of the minimal assessment of cognitive function in multiple sclerosis (MACFIMS). *J Int Neuropsychol Soc* 2006;12:549–558.
- Cutter GR, Baier ML, Rudick RA, et al. Development of a multiple sclerosis functional composite as a clinical trial outcome measure. *Brain* 1999;122(Pt 5):871–882.
- Drake AS, Weinstock-Guttman B, Morrow SA, et al. Psychometrics and normative data for the Multiple Sclerosis Functional Composite: replacing the PASAT with the Symbol Digit Modalities Test. *Mult Scler* 2010;16:228–237.
- Huang SY, Witzel T, Fan Q, et al. TractCaliber: Axon diameter estimation across white matter tracts in the in vivo human brain using 300 mT/m gradients. *Proceedings of the 23rd Annual Meeting of the ISMRM; Toronto, Canada. 2015.*
- Fan Q, Witzel T, Nummenmaa A, et al. MGH-USC Human Connectome Project datasets with ultra-high b-value diffusion MRI. *NeuroImage* 2016;124(Pt B):1108–1114.
- Fischl B. *FreeSurfer*. *NeuroImage* 2012;62:774–781.
- Smith SM, Jenkinson M, Woolrich MW, et al. Advances in functional and structural MR image analysis and

- implementation as FSL. *NeuroImage* 2004;23(Suppl 1): S208–S219.
27. Alexander DC, Hubbard PL, Hall MG, et al. Orientationally invariant indices of axon diameter and density from diffusion MRI. *NeuroImage* 2010;52:1374–1389.
 28. Fan Q, Nummenmaa A, Wichtmann B, et al. Validation of diffusion MRI estimates of compartment size and volume fraction in a biomimetic brain phantom using a human MRI scanner with 300 mT/m maximum gradient strength. *NeuroImage* 2018;182:469–478.
 29. Fan Q, Tian Q, Ohringer NA, et al. Age-related alterations in axonal microstructure in the corpus callosum measured by high-gradient diffusion MRI. *NeuroImage* 2019;191:325–336.
 30. Alexander DC. A general framework for experiment design in diffusion MRI and its application in measuring direct tissue-microstructure features. *Magn Reson Med* 2008;60:439–448.
 31. Huang SY, Tobyne SM, Nummenmaa A, et al. Characterization of axonal disease in patients with multiple sclerosis using high-gradient-diffusion MR imaging. *Radiology* 2016;9:151582.
 32. Dale AM, Fischl B, Sereno MI. Cortical surface-based analysis. I. Segmentation and surface reconstruction. *NeuroImage* 1999;9:179–194.
 33. Fischl B, Sereno MI, Dale AM. Cortical surface-based analysis. II: Inflation, flattening, and a surface-based coordinate system. *NeuroImage* 1999;9:195–207.
 34. Tobyne SM, Boratyn D, Johnson JA, et al. A surface-based technique for mapping homotopic interhemispheric connectivity: development, characterization, and clinical application. *Hum Brain Mapp* 2016;37:2849–2868.
 35. Klawiter EC, Ceccarelli A, Arora A, et al. Corpus callosum atrophy correlates with gray matter atrophy in patients with multiple sclerosis. *J Neuroimaging* 2015;25:62–67.
 36. Jenkinson M, Bannister P, Brady M, Smith S. Improved optimization for the robust and accurate linear registration and motion correction of brain images. *NeuroImage* 2002;17:825–841.
 37. Zhang Y, Brady M, Smith S. Segmentation of brain MR images through a hidden Markov random field model and the expectation-maximization algorithm. *IEEE Trans Med Imaging* 2001;20:45–57.
 38. Nedjati-Gilani GL, Schneider T, Hall MG, et al. Machine learning based compartment models with permeability for white matter microstructure imaging. *NeuroImage* 2017;15:119–135.
 39. Bergers E, Bot JC, De Groot CJ, et al. Axonal damage in the spinal cord of MS patients occurs largely independent of T2 MRI lesions. *Neurology* 2002;59:1766–1771.
 40. Bergers E, Bot JC, van der Valk P, et al. Diffuse signal abnormalities in the spinal cord in multiple sclerosis: direct postmortem in situ magnetic resonance imaging correlated with in vitro high-resolution magnetic resonance imaging and histopathology. *Ann Neurol* 2002;51:652–656.
 41. Waxman SG. Ions, energy and axonal injury: towards a molecular neurology of multiple sclerosis. *Trends Mol Med* 2006;12:192–195.
 42. Mahad DJ, Ziabreva I, Campbell G, et al. Mitochondrial changes within axons in multiple sclerosis. *Brain* 2009;132 (Pt 5):1161–1174.
 43. Yaldizli O, Penner IK, Frontzek K, et al. The relationship between total and regional corpus callosum atrophy, cognitive impairment and fatigue in multiple sclerosis patients. *Mult Scler* 2014;20:356–364.
 44. Dutta R, Trapp BD. Mechanisms of neuronal dysfunction and degeneration in multiple sclerosis. *Prog Neurobiol* 2011;93:1–12.
 45. Burcaw LM, Fieremans E, Novikov DS. Mesoscopic structure of neuronal tracts from time-dependent diffusion. *NeuroImage* 2015;01:18–37.
 46. Lee HH, Fieremans E, Novikov DS. What dominates the time dependence of diffusion transverse to axons: intra- or extra-axonal water? *NeuroImage* 2018;15:500–510.
 47. Novikov DS, Jensen JH, Helpert JA, Fieremans E. Revealing mesoscopic structural universality with diffusion. *Proc Natl Acad Sci USA* 2014;111:5088–5093.
 48. De Santis S, Jones DK, Roebroeck A. Including diffusion time dependence in the extra-axonal space improves in vivo estimates of axonal diameter and density in human white matter. *NeuroImage* 2016;15:91–103.
 49. Fieremans E, Burcaw LM, Lee HH, et al. In vivo observation and biophysical interpretation of time-dependent diffusion in human white matter. *NeuroImage* 2016;01:414–427.